Theor Chem Acc (2005) 114: 90–96
DOI 10.1007/s00214-005-0648-x

REGULAR ARTICLE

G.M. Zhidomirov · A.A. Shubin · V.B. Kazansky
R.A. van Santen

Spectroscopic identification of adsorption properties of Zn^{2+} ions at cationic positions of high-silica zeolites with distant placing of aluminium ions

Received: 15 August 2004 / Accepted: 13 December 2004 / Published online: 12 May 2005

Abstract For Zn^{2+} cations in ZnZSM-5 zeolite unusual type of cationic positions, formed by two distantly placed framework aluminium atoms, is considered. Some extent of structural destabilization of cations in these cationic positions in comparison with traditional localization should result in promoted Lewis activity and adsorption activity of these sites. The last ones are manifested in the significantly increased IR low frequency shifts for adsorbed molecules and in their ability for heterolytic dissociation at elevating temperature. DFT cluster quantum chemical modeling of light alkane adsorption on Zn^{2+} in ZnZSM-5 zeolites confirms these conjectures in full agreement with recent experiments. Similar to the previously considered dihydrogen and methane molecule adsorption, we present here the calculations of ethane molecular and dissociative adsorption on these sites. It is shown that the unusually large ethane IR frequency shift recently observed in ZnZSM-5 zeolite can result from adsorptive interaction of C_2H_6 with Zn^{2+} stabilized in a cationic position with distantly placed aluminium ions. The dissociative adsorption of ethane molecules with the formation of bridged hydroxyl group and Zn–C_2H_5 structure is considered and an activation energy of ethylene formation from the alkyl fragment is evaluated.

Keywords Ethane · Adsorption · Heterolytic dissociation · ZnZSM-5 zeolites · DFT

1 Introduction

Zinc-containing high-silica zeolites are known as an effective catalysts for dehydrogenation and aromatization of light alkanes [1–3]. Significant efforts have been devoted to clear up the role of Zn-active components during these processes [3–5]. At present, there is the consensus that zinc cationic species are essentially important for acceleration of paraffin dehydrogenation – the first step of alkanes' aromatization reaction. In principle, different cites of Zn^{2+} ion stabilization in zeolites can be realized: stabilization in the small (4–6)-membered zeolite rings with two aluminium atoms in the ring, the binuclear $[Zn–O–Zn]^{2+}$ structures, and the extra-framework zinc oxide clusters $(ZnO)_n$. Relative appearance of these forms should depend on the zeolite type and its Si/Al module, zinc loading, the procedure of active component introduction, and on subsequent thermo-chemical treatment [6]. Comparison of the activity of these forms in the dehydrogenation of alkanes is important for understanding the catalytic properties of Zn high-silica zeolites. Most research suggests the main role of Zn^{2+} ion species in cationic positions of zeolites [3–5, 7]. Theoretical study of the reaction path of ethane dehydrogenation on Zn^{2+} cation stabilized in four-membered zeolitic ring was carried out in [7]. It was concluded that the "alkyl" path of ethane activation is most probable, while the first step of this process should be heterolytic dissociation of C_2H_6 into $C_2H_5^-$ and H^+. This step in the reaction of ethane molecule on Zn^{2+} ion placed at various ring cationic positions of ZSM-5 zeolite has been considered in [8]. Qualitative correlation between decreased stability of the zinc cation in the cationic sites and increased activity of these sites in the reaction was found. Stabilization energy (*Est*) of Zn^{2+} has been evaluated as the enthalpy of the reaction

$$Zn^{2+}/Z + H_2 = Zn^0 + 2H^+/Z, \tag{1}$$

where 2 H^+ / Z is the hydrogen form of the cationic position. Generally speaking, there are two main factors responsible for the destabilization of cation position and increase in the

G.M. Zhidomirov (✉) · A.A. Shubin
Boreskov Institute of Catalysis,
Siberian Branch of the Russian Academy of Sciences,
(Pr. Akad. Lavrentieva 5), Novosibirsk 630090, Russia
E-mail: Zhi@catalysis.nsk.su

V.B. Kazansky
Zelinsky Institute of Organic Chemistry of Russian Academy of Sciences, (Leninsky prospect 47), Moscow 117913, Russia

R.A. van Santen
Schuit Institute of Catalysis, Eindhoven University of Technology, P.O. Box 513, 5600 MB, Eindhoven, The Netherlands

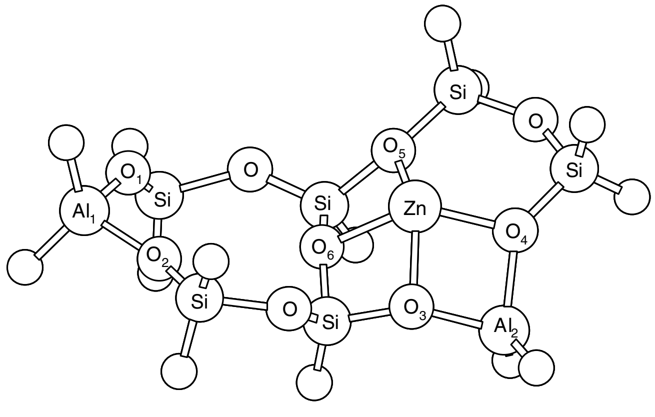

Fig. 1 Structure **I**. The suggested active site with two distantly separated Al lattice ions placed in different zeolite rings

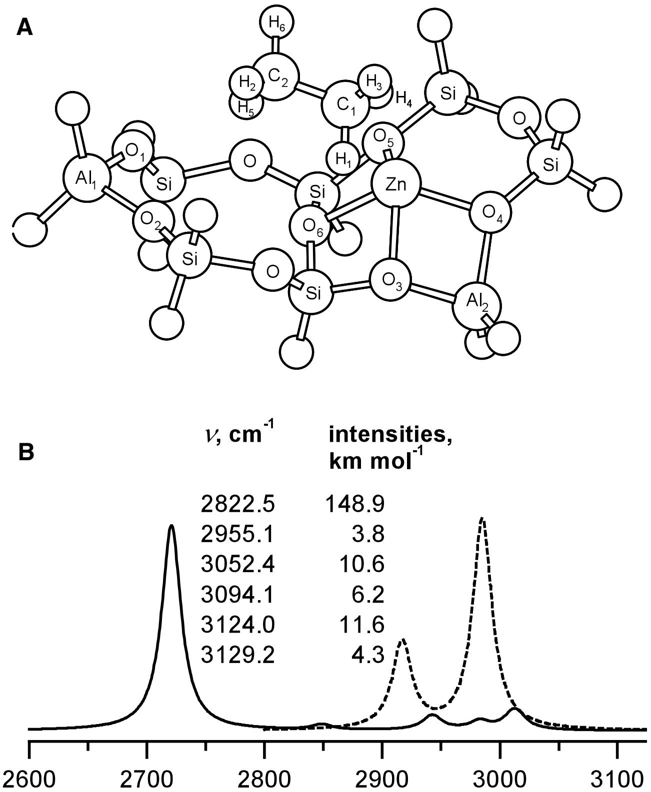

Fig. 2 Structure **II**. **a** First strong adsorption form for ethane molecule. **b** Calculated IR frequencies with their intensities and simulated IR spectrum (with all DFT computed vibrational frequencies scaled by factor 0.964) for this structure. IR spectrum of free C_2H_6 molecule calculated at the same DFT level is presented for comparison by the *dashed line*

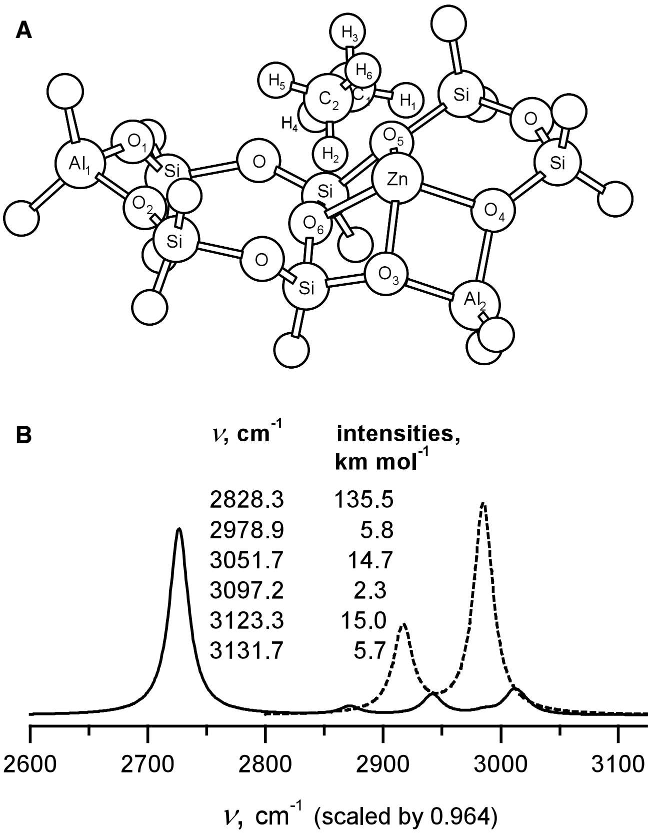

Fig. 3 Structure **III**. **a** Second strong adsorption form for ethane molecule. **b** Calculated IR frequencies with their intensities and simulated IR spectrum (scaled as in Fig. 2) for this structure

Lewis acidity of the Zn^{2+}: steric hindrance of the cation adsorption due to the structural peculiarities of the site and the decrease in adsorption interaction, which could be associated with mutual sitting of two aluminium charge compensating ions in the zeolite lattice. An example of the first one is Zn^{2+} stabilized in a four-membered zeolite ring in comparison with Zn^{2+} stabilized in a five-membered ring [8]. The importance of the second of these factors became clear after recent DRIFT studies of H_2 [9, 10] and CH_4 [11] adsorption on ZnZSM-5 zeolites with various zeolite modules. It was concluded that stabilization of two-valent Zn^{2+} cation at one aluminium ion is possible with distant placing of the second charge compensating aluminium ion. Unusually large red frequency shifts were found for adsorbed H_2 (220–230 cm^{-1}) and CH_4 (110 cm^{-1}) molecules. In addition, their heterolytic dissociation was observed after a moderate elevation in temperature [9–11]. All of these data were explained by promoted activation of adsorbed molecules on the above mentioned unusually strong Lewis active sites with distantly placed aluminium ions. Theoretical studies [12, 13] confirm such suggestion. Earlier [14], a zeolite fragment with distantly placed (more than 7.5 Å) two-lattice aluminium ions was also considered as a cation position for the stabilization of binuclear form $[Zn–O–Zn]^{2+}$. Such a binuclear structure with extralattice oxygen has been identified in [6] and

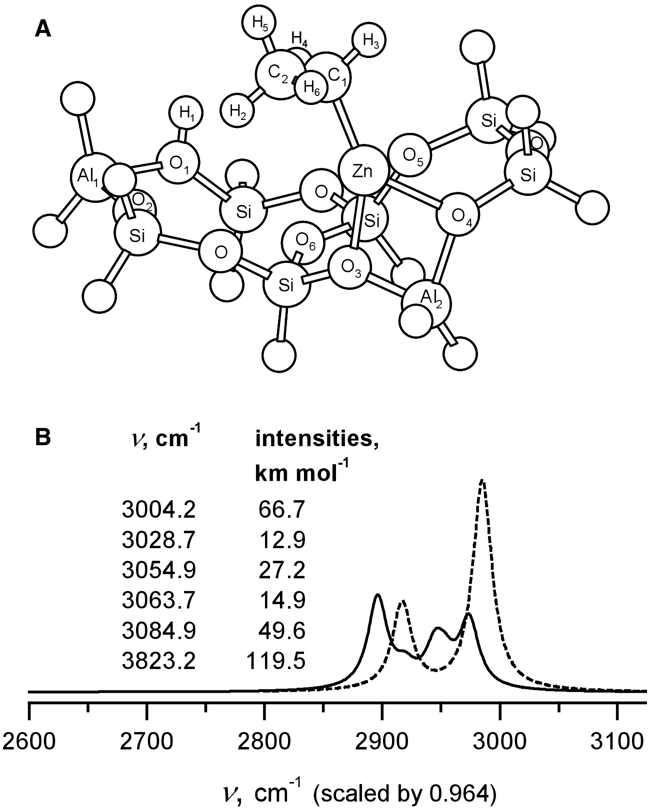

ν, cm^{-1}	intensities, km mol^{-1}
3004.2	66.7
3028.7	12.9
3054.9	27.2
3063.7	14.9
3084.9	49.6
3823.2	119.5

Fig. 4 Structure **IV**. **a** First dissociative adsorption form for ethane molecule. **b** Calculated IR frequencies with their intensities and simulated IR spectrum(scaled as in Fig. 2) for this structure

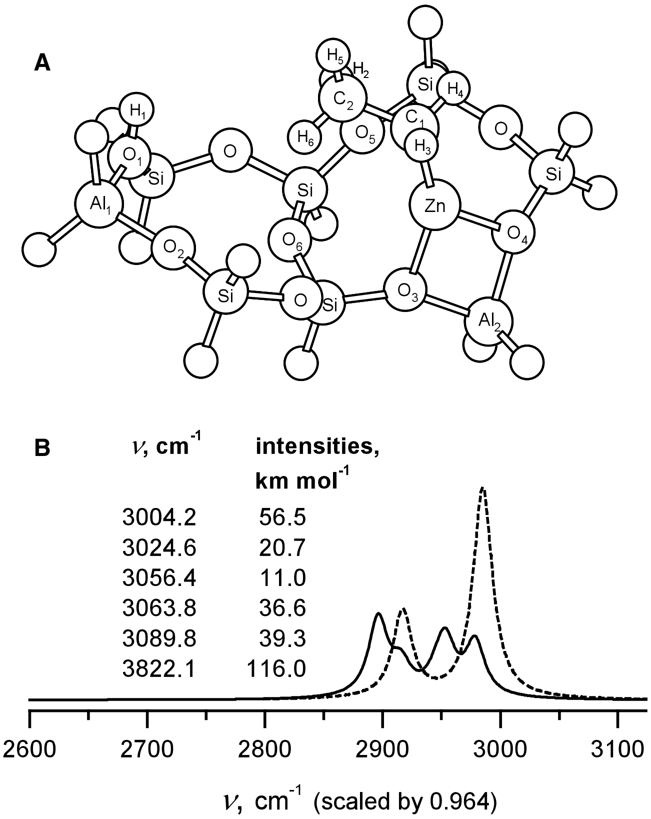

ν, cm^{-1}	intensities, km mol^{-1}
3004.2	56.5
3024.6	20.7
3056.4	11.0
3063.8	36.6
3089.8	39.3
3822.1	116.0

Fig. 5 Structure **V**. **a** Second dissociative adsorption form for ethane molecule. **b** Calculated IR frequencies with their intensities and simulated IR spectrum(scaled as in Fig. 2) for this structure

suggested in [3] to account for the overexchange phenomena in the zinc exchanged zeolites. Simultaneously, we demonstrated in [14] the possibility of single Zn^{2+} ion stabilization in such cationic positions (the last one was termed as Z_dZn) and discussed the unusual chemical properties of this site. Lowering stability and high reactivity of these cationic positions were revealed, but the study of H_2 and CH_4 adsorption and perturbation of their IR frequency bands were not carried out. Such calculations have been subsequently performed and a large adsorption low-frequency shift ($-254\,cm^{-1}$) for the stretching vibration band of H_2 [12] and abnormally high-frequency shift ($-107\,cm^{-1}$) of symmetric (A_1) stretching band of CH_4 molecule have been found [13]. It has been shown earlier that such large shift of vibration frequencies could not be explained for H_2 [15] and CH_4 [16] by interaction of these molecules with traditional forms of zinc ion species in high-silica zeolites. At the same time, calculations showed that Zn^{2+} ions in the cationic positions considered here can produce large perturbations of IR vibration frequencies of adsorbed molecules in agreement with experiments. We suggest that it is important confirmation of the reliability of cationic positions with distantly placed lattice aluminium ions for two-valent metal ions [10].

Recently, a DRIFT study of ethane adsorption and dehydrogenation on ZnZSM-5 zeolite has been performed [17]. In parallel to a similar study for methane [11], besides an observation of weak adsorption species, strong ethane adsorption form was found. This form has very intensive broad IR band and a frequency which is more than $200\,cm^{-1}$ lower than those of the C–H stretching vibrations of gaseous or physically adsorbed ethane molecules. Heterolytic dissociation of this strong adsorption form initiated by the increase in temperature results in a zinc ethyl fragment and acid-bridged hydroxyl group. Subsequent elevation in the temperature gives rise to the decomposition of ethyl fragment and to the formation of zinc hydride and ethylene. Here, we are going to show that cluster model DFT calculations of adsorbed and dissociated forms of ethane molecule on Z_dZn site are in agreement with the above cited [17] DRIFT study of the strongly adsorbed ethane species. In this work, we use the same cluster model of Z_dZn site as in previous studies of H_2 [12] and CH_4 [13] adsorption.

2 Computation details

Two adjacent five-rings on the wall of the straight channel of ZSM-5 zeolite have been suggested as a possible cationic site for the zinc ion with Al atoms placed in T_{12} and T_8 lattice positions [20]. The $ZnAl_2Si_6O_9H^*_{14}$ was chosen for subsequent DFT modeling. The quantum chemical computations were carried out within the gradient-corrected density

Table 1 Some atom-atom distances for calculated structures **I-IX**[a]

	I	II	III	IV	V	VI	VII	VIII	IX
Zn–$O_{(3)}$	1.973	2.014	2.003	1.973	1.971	1.974	1.981	2.022	1.951
Zn–$O_{(4)}$	1.916	1.952	1.957	2.022	2.021	2.020	2.010	2.041	1.995
Zn–$O_{(5)}$	2.019	2.112	2.090	3.516	3.436	3.540	3.985	3.796	3.467
Zn–$O_{(6)}$	2.081	2.133	2.142	3.544	3.511	3.552	3.777	3.686	3.522
Zn–$C_{(1)}$		2.388	2.400	1.940	1.941	1.942	2.055	2.529	
Zn–$C_{(2)}$		3.475	3.465	2.881	2.912	2.942	2.151	2.453	
Zn–$H_{(2)}$							1.686	1.541	1.513
$O_{(1)}$–$H_{(1)}$				0.965	0.966	0.965	0.965	0.966	0.965
$C_{(1)}$–$C_{(2)}$		1.532	1.529	1.537	1.536	1.535	1.432	1.339	

[a] For isolated C_2H_6 and C_2H_4 molecules computed at B3LYP DFT level with 6-311G** basis set, C–C distances are 1.530 Å and 1.327 Å, respectively

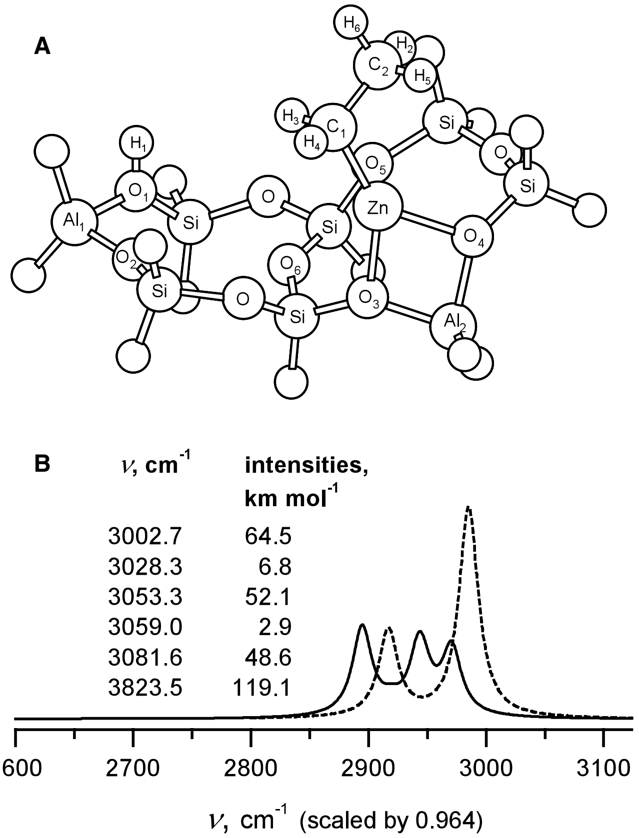

ν, cm^{-1}	intensities, km mol^{-1}
3002.7	64.5
3028.3	6.8
3053.3	52.1
3059.0	2.9
3081.6	48.6
3823.5	119.1

Fig. 6 Structure **VI**. **a** Third dissociative adsorption form for ethane molecule. **b** Calculated IR frequencies with their intensities and simulated IR spectrum(scaled as in Fig. 2) for this structure

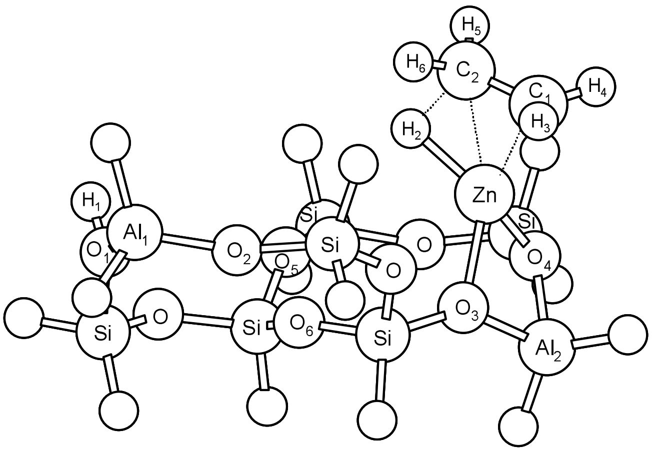

Fig. 7 Structure **VII**. The transition state structure for β-H transfer to the Zn ion. This transition state connects structure **VI** with structure **VIII**

functional theory (DFT) using the GAUSSIAN-98 program [18]. In the present study, a B3LYP functional was used to estimate electron exchange and correlation contributions to energy. It contains the Hartree–Fock exchange, the mixture of exchange and correlation functionals including gradient corrections of the electron density, and the carefully chosen empirical parameters that have been obtained from fitting the calculated results to the accurate experimental data. Nowadays, such a hybrid B3LYP method is very often used in chemical applications [19]. This approach was also rather successful in our earlier studies of Zn containing zeolites [12, 13]. In the course of simulation of C_2H_6 interaction with a zinc ion at the zeolite cationic position, the 6-31G* basis set was used for zinc and 6-311G** basis set for the C_2H_6, the zeolite oxygen atoms, and the hydrogen atoms of the bridging hydroxyl groups. Al and Si atoms of the zeolite framework, as well as (H*) hydrogen atoms saturating the broken Si–O bonds, were treated by the D95-Dunning/Huzinaga basis set. Such a compromised choice allowed us to save computational time and, at the same time, to use the extended models for the frequency calculations without significant loss of accuracy.

Special restrictions were imposed on the optimization of positions of the boundary H* atoms. At the first step of the optimization procedure, the geometry of $ZnAl_2Si_6O_9H^*_{14}$ zeolite cluster was fixed according to experimental X-ray diffraction data [20]. Only Si-H* and Al–H* bond distances were optimized, while the positions of other atoms (except Zn), as well as directions of O–H* bonds, were kept fixed according to crystallographic data. The Zn^{2+} ion was allowed to move freely in the zeolite structure. Subsequent second step of optimization was performed with fixed positions of H* atoms. Positions of H* atoms obtained for $ZnAl_2Si_6O_9H^*_{14}$ cluster after the first step of this optimization procedure were saved and kept fixed in the subsequent restricted geometry optimizations of H-forms and other zeolite structures with

Table 2 Mulliken charges for calculated structures **I–IX**[a]

	I	II	III	IV	V	VI	VII	VIII	IX
Zn	0.984	0.953	0.933	0.797	0.818	0.799	0.777	0.618	0.660
$Al_{(1)}$	1.067	1.082	1.068	1.096	1.098	1.095	1.096	1.095	1.095
$Al_{(2)}$	1.157	1.157	1.146	1.143	1.151	1.149	1.158	1.133	1.131
$O_{(1)}$	−1.061	−1.075	−1.067	−0.896	−0.898	−0.896	−0.897	−0.899	−0.896
$O_{(2)}$	−1.110	−1.122	−1.110	−1.148	−1.156	−1.149	−1.148	−1.146	−1.149
$O_{(3)}$	−1.149	−1.148	−1.150	−1.169	−1.170	−1.171	−1.168	−1.178	−1.176
$O_{(4)}$	−1.138	−1.143	−1.145	−1.152	−1.153	−1.150	−1.144	−1.154	−1.160
$O_{(5)}$	−1.139	−1.144	−1.143	−1.093	−1.100	−1.093	−1.084	−1.086	−1.093
$O_{(6)}$	−1.149	−1.160	−1.155	−1.115	−1.117	−1.114	−1.114	−1.114	−1.113
$C_{(1)}$		−0.416	−0.428	−0.535	−0.543	−0.541	−0.489	−0.256	
$C_{(2)}$		−0.301	−0.284	−0.300	−0.307	−0.285	−0.252	−0.303	
$H_{(1)}$		0.162	0.101	0.363	0.364	0.363	0.363	0.365	0.363
$H_{(2)}$		0.138	0.153	0.114	0.101	0.089	−0.192	−0.172	−0.131
$H_{(3)}$		0.165	0.170	0.106	0.115	0.112	0.142	0.174	
$H_{(4)}$		0.071	0.154	0.112	0.104	0.117	0.137	0.158	
$H_{(5)}$		0.175	0.146	0.102	0.100	0.104	0.169	0.150	
$H_{(6)}$		0.121	0.120	0.101	0.111	0.104	0.177	0.163	

[a] For isolated C_2H_6 molecule computed at B3LYP DFT level with 6–311G** basis set, C–C Mulliken charges are −0.317 and 0.106 for C and H atoms, respectively. For isolated C_2H_4 molecule, corresponding charges are –0.219 and 0.109

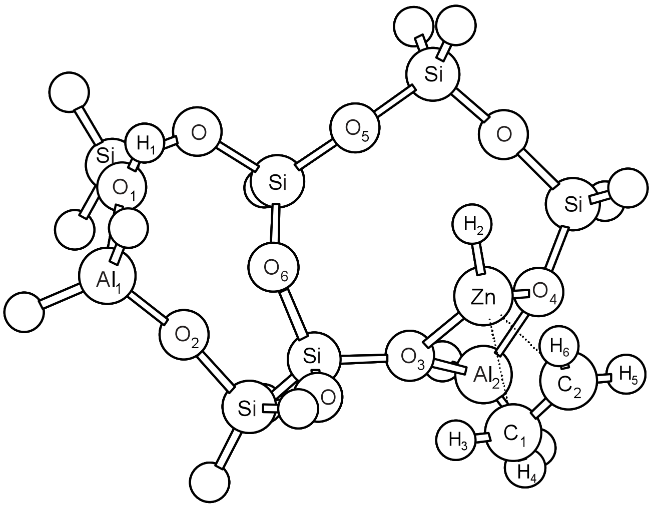

Fig. 8 Structure **VIII.** The first product (which contains zinc hydride and adsorbed ethylene) of β-H transfer to the Zn ion reaction for structure **VI**

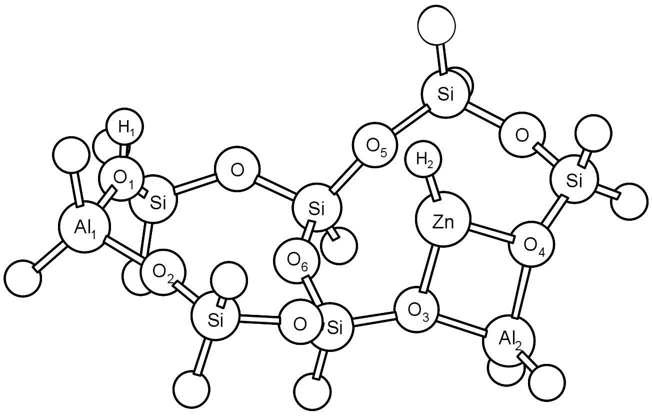

Fig. 9 Structure **IX.** The result of ethylene desorption from structure **VIII**

two connected 5-membered rings. For calculation of vibrational frequencies, all bond saturating H* atoms were released but their masses were set to a very large value (1000000).

3 Results and discussion

The cluster model of the active site with two distantly separated lattice Al atoms, which are placed in two adjacent zeolite rings, is shown in Fig. 1. Zn^{2+} ion is localized near $Al_{(2)}$ atom with the Zn–$Al_{(2)}$ distance equal to 2.866 Å and a rather long Zn–$Al_{(1)}$ distance to the second aluminum atom of 6.170 Å. The most interesting interatomic distances and Mulliken charges for this and subsequent structures are collected in Tables 1 and 2, respectively. It is evident from these results that Zn is coordinated by four most closely surrounding oxygen atoms with slightly shorter distances to two of them bounded to $Al_{(2)}$. Two forms of ethane adsorption that are shown in Figs. 2 and 3 by structures **II** and **III** correspond to two local minima with very close adsorption energies. They can be approximately converted to each other by rotation of ethane molecules around the Zn–$C_{(1)}$ bond. The adsorption energies for both structures are equal to 13.4 and 12.2 kcal/mol, respectively, with the small preference of structure **II**. After ethane adsorption, the fourfold coordination of Zn by the lattice oxygen atoms remains unchanged; however, all four Zn–O distances became somewhat longer (see Figs. 2, 3 and Table 1). Effective transfer of electron density from ethane to the adsorption site is equal to 0.115 electron that is in agreement with the slight decrease in the positive charge of Zn ion (Table 2). This indicates appreciable Lewis acidity of the considered active site involving the Zn^{+2} ion in a cationic position with distantly placed aluminum ions. It was shown earlier [14] that such peculiarity of active site really promotes its Lewis acidity. The electron transfer to Zn^{2+} from adsorbed ethane is about 0.015 electron

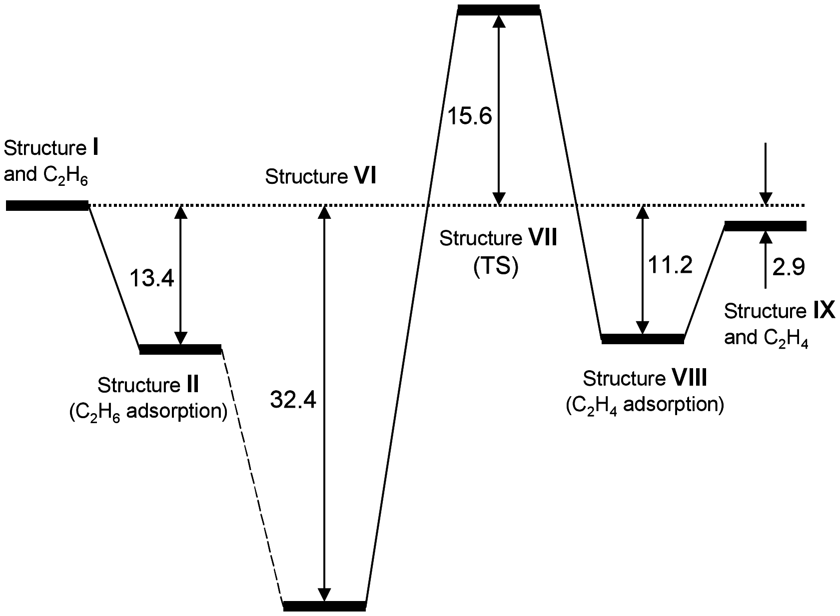

Fig. 10 Reaction energy diagram of ethylene formation. Reaction path (shown in dash) between structure **II** and structure **VI** should include several additional steps (not shown in this figure) corresponding to heterolytic dissociation of C_2H_6 and subsequent proton migration similar to those considered in [12] for H_2. All values in kcal/mol

larger than for the previously studied methane adsorption [13]. Ethane adsorption also results in strong polarization of adsorbed molecules and in significant change in charge distribution resulting from interaction with zinc cations (see Table 2).

The calculated C–H stretching frequencies of adsorbed ethane and intensities of corresponding IR bands are indicated in Figs. 2, 3. The simulated IR spectra carried out using the scaled 0.964 calculated frequencies are shown in these figures by the solid lines, while the corresponding IR bands are slightly artificially broadened. For comparison purposes, scaled in the same manner, IR spectrum of free ethane molecules (shown by the broken line) was also calculated at the same DFT level.

The most remarkable feature of the calculated spectra of the strong molecular form of ethane adsorption is the very intense lines at 2720 cm^{-1} for structure **II** and at 2726 cm^{-1} for structure **III** that are very strongly red shifted in comparison with the spectrum of the free ethane. Positions and intensities of these lines are in good agreement with those for the experimentally observed most strongly red-shifted IR band at 2727 cm^{-1} in the experimentally observed spectrum of the strong molecular form of ethane adsorption reported in [17]. Several much weaker C–H stretching bands that were observed in [17] in the region of 2800–3000 cm^{-1} are also associated with this form of adsorption. According to our calculations for structure **II**, their scaled frequencies are at the following: 2849, 2942, 2982, 3010, and 3016 cm^{-1} positions (see Fig. 2). The calculated spectrum of structure **III** is quite similar with the only exception that the band at 2872 cm^{-1} for structure **II** was shifted to 2848 cm^{-1} for structure **III**. The calculated IR spectra in general quite nicely fit the experimental results, with the only exception for the 2816 cm^{-1} band that is absent in the theoretical spectra. This discrepancy is most likely connected with contribution to the experimentally observed spectrum of a weaker form of ethane adsorption.

Heating of a ZnZSM-5 zeolite with adsorbed ethane at 423 K destroys the strong molecular form of ethane adsorption. Instead, it results in heterolytic dissociation of ethane with the formation of a Zn–ethyl fragment and the bridging hydroxyl group [17]. We were able to find at least three different isomers of dissociatively adsorbed ethane with practically the same total energies. They are presented in Figs. 4, 5, and 6.

As follows from these figures, dissociation of the strong form of molecular ethane adsorption results in the formation of Zn–C bonds with simultaneous weakening of two weaker Zn–O bonds with $Al_{(2)}$ atom (see Table 1). Reduction of the active site makes itself evident in an appreciable decrease in the positive charge of Zn ion (Table 2). The calculated C–H stretching frequencies for all of dissociated structures **IV**, **V**, and **VI** are very similar and are in a reasonable agreement with those experimentally observed. For example, for structure **IV** in Fig. 4 they are equal to 2896 cm^{-1}, 2920 cm^{-1} and several much weaker bands at 2944, 2954, 2974 cm^{-1}, while the experimentally observed vibrational frequencies reported in Ref. [17] are equal to 2874, 2958 and 2010 cm^{-1}.

Prolonged evacuation of the sample with the dissociatively adsorbed ethane at 523 K results in the formation of ethylene and in appearance of a Zn–H bond with the stretching frequency of 1934 cm^{-1} [17]. We considered the β-H transfer to the Zn ion as is presented by structure **VI**. The calculated geometry of the corresponding transition state is shown in Fig. 7. The estimated activation energy of 48.0 kcal/mol seems to be rather reasonable. During the formation of such TS, the Zn–$C_{(1)}$ and Zn–$C_{(2)}$ bond distances are equalized, while the C–C bond becomes shorter by 0.1 Å and a new Zn–H bond with hydride character is forming (see in this connection structure **VII** in Fig. 7 and Tables 1 and 2). The first product of the reaction is structure **VIII** (Fig. 8), which contains zinc hydride and adsorbed ethylene coordinated by the π- bonding with the zinc ion. The energy of this structure is by 26.8 kcal/mol lower than that of the transition state **VII**.

Desorption of ethylene results in structure **IX** (Fig. 9), which contains the bridging hydroxyl group and the zinc hydride group. The calculated desorption energy of ethylene is equal to 8.3 kcal/mole, while the calculated Zn–H stretch frequency of 1881 cm^{-1} is in reasonable agreement with the experimental value of 1934 cm^{-1}. It is quite remarkable that adsorption of ethylene (structure **VIII**) decreased the Zn–H frequency to 1788 cm^{-1}. The reaction energy diagram summarizing results of calculations for some structures is presented in Fig. 10.

4 Conclusion

An unusual type of localization in high-silica zeolites of bivalent metal ions at two distantly separated lattice aluminum atoms was considered. The consecutive stages of ethane dehydrogenation by these sites, including the strong molecular adsorption, of ethane, its subsequent heterolytic dissociative adsorption, and ethylene formation via splitting of hydride ions from ethyl fragments, were analyzed via DFT cluster calculations. The obtained results indicated that the unusually large low-frequency shift of stretching frequency of one of IR C–H stretching bands that was recently observed for ethane adsorption by a ZnZSM-5 zeolite is connected with perturbation of C_2H_6 by Zn^{2+} ions at such sites with promoted Lewis acidity. At least, two possible molecular adsorption forms and three heterolytically dissociated structures were found. C–H vibrational frequencies for all these reaction intermediates were calculated. They are in reasonable agreement with the experimental results.

Acknowledgements The authors are grateful to NWO and RFBR for the financial support of this work in the frame of Russian-Dutch scientific cooperation, Grant 047-015-001. G.M.Z and A.A.S thank the Program for Science School support (project SS-1140.2003.3), and V.B.K thanks the Program for Science School support (project SS-1745.2003.3) and the Program of Department of Chemistry and Material Science of RAS.

References

1. Mole T, Anderson JR, Creer G (1985) Appl Catal 17:127–140
2. Ono Y, (1992) Catal Rev Sci Eng 34:179–226
3. Biscardi JA, Meitzner GD, Iglesia EJ (1998) J Catal 179:192–202
4. Kumar N, Lindfors LE (1996) Catal Lett 38:239–244
5. Biscardi JA, Iglesia EJ (1996) Catal Today 31:207–231
6. Pensien J, Abraham A, van Bokhoven JA, Jentys A, Miller TE, Sievers C, Lercher JA (2004) J Phys Chem B 108:4116–4126
7. Frash MV, van Santen RA (2000) PCCP 2:1085–1089
8. Shubin AA, Zhidomirov GM, Yakovlev AL, van Santen RA (2001) J Phys Chem B 105:4928–4935
9. Kazansky VB, Serikh AI (2004) Micropor Mesopor Mater 70:151–154
10. Kazansky VB (2003) J Catal 216:192–202
11. Kazansky VB, Serikh AI, Pidko EA (2004) J Catal 225:369–373
12. Shubin AA, Zhidomirov GM, Kazansky VB, van Santen RA (2003) Catal Lett 90:137–142
13. Zhidomirov GM, Shubin AA, Kazansky VB, van Santen RA (2004) Int Journ Quant Chem 100:489–494
14. Yakovlev AL, Shubin AA, Zhidomirov GM, van Santen RA (2000) Catal Lett 70:175–181
15. Barbosa LAMM, Zhidomirov, GM, van Santen RA (2001) Catal Lett 77:55–62
16. Barbosa LAMM, Zhidomirov GM, van Santen RA (2000) PCCP 2:3909–3918
17. Kazansky VB, Pidko EA (2004) J Phys Chem B online publication
18. Gaussian 98, Revision A.11, Frisch MJ, Trucks GW, Schlegel HB, Scuseria GE, Robb MA, Cheeseman JR, Zakrzewski VG, Montgomery JA Jr, Stratmann RE, Burant JC, Dapprich S, Millam JM, Daniels AD, Kudin KN, Strain MC, Farkas O, Tomasi J, Barone V, Cossi M, Cammi R, Mennucci B, Pomelli C, Adamo C, Clifford S, Ochterski J, Petersson GA, Ayala PY, Cui Q, Morokuma K, Salvador P, Dannenberg JJ, Malick DK, Rabuck AD, Raghavachari K, Foresman JB, Cioslowski J, Ortiz JV, Baboul AG, Stefanov BB, Liu G, Liashenko A, Piskorz P, Komaromi I, Gomperts R, Martin RL, Fox DJ, Keith T, Al-Laham MA, Peng CY, Nanayakkara A, Challacombe M, Gill PMW, Johnson B, Chen W, Wong MW, Andres JL, Gonzalez C, Head-Gordon M, Replogle ES, Pople JA (2001) Gaussian Inc., Pittsburgh
19. Baker J, Muir M, Andzelm J, Scheiner A (1996) In: Laird BB, Ross RB, Ziegler T, (eds). Chemical applications of density-functional theory, ACS symposium series 629. American Chemical Society, Washington
20. Lermer H, Draeger M, Steffen J, Unger KK (1985) Zeolites 5:131–134